CU-CAS-02-25

CENTER FOR AEROSPACE STRUCTURES

Fitting Strains and Displacements by Minimizing Dislocation Energy

by

C. A. Felippa

December 2002

COLLEGE OF ENGINEERING
UNIVERSITY OF COLORADO
CAMPUS BOX 429
BOULDER, COLORADO 80309

Fitting Strains and Displacements by Minimizing Dislocation Energy

C. A. Felippa and K. C. Park

Department of Aerospace Engineering Sciences
and Center for Aerospace Structures
University of Colorado, Campus Box 429
Boulder, Colorado 80309-0429, USA

Report No. CU-CAS-02-25

June 2002, revised December 2002

Presented at the Sixth International Conference on Computational Structures Technology, held at Prague, Czech Republic, September 2002. Proceedings made available only in CD-ROM.

Fitting Strains and Displacements by Minimizing Dislocation Energy

Carlos A. Felippa* and K. C. Park

Department of Aerospace Engineering Sciences
and Center for Aerospace Structures
University of Colorado at Boulder
Boulder, Colorado 80309-0429, USA
* Corresponding author
e-mail: carlos@titan.colorado.edu, web page: http://caswww.colorado.edu

Abstract

We present a procedure for matching a displacement field to a given strain field, or vice-versa, over an arbitrary domain, which can be a finite element. The fitting criterion used is minimization of a dislocation energy functional. The strain field, whether given or fitted, need not be compatible. The method has four immediate applications: (i) finite element stiffness formulation based on fitting assumed-natural-strain (ANS) fields to node displacements; (ii) pointwise recovery of an internal displacement field in ANS elements as required for consistent mass, body load or geometric stiffness computations; (iii) recovery of smoothed strains from node displacements for stress post-processing, and (iv) system identification and damage detection from experimental data. The article focuses on application (i) for the strain fitting (SF) problem and (ii) for the displacement fitting (DF) problem. The separation of mean and deviatoric strains is emphasized whenever it is found convenient to simplify calculations.

Keywords: finite element methods, dislocation energy minimization, strain fitting, displacement fitting, strain-assumed elements, straingages, individual element test.

1 Background

Consider a linear elastic body of volume V and surface S with exterior normal $\mathbf{n}$, referred by a position vector $\mathbf{x}$, as illustrated in Figure 1. Anticipating application to individual finite elements in a stiffness-based implementation, the body will be taken to be fully unconstrained. Thus the only boundary conditions over S are of traction type.

1.1 The Fitting Problems

We are given the strain field

$$\mathbf{e}(\mathbf{x}) \quad \text{in} \quad V. \tag{1}$$

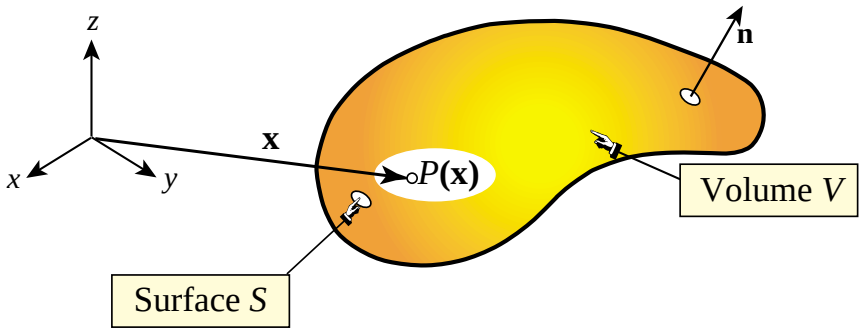

Figure 1. Body of volume V and boundary S for posing the DF and SF problems.

which contains free or specified parameters. Free parameters could be point values akin to straingage readings, in which case we call (1) a *gaged field*.

The components of $\mathbf{e}$ are arranged in vector form in the usual manner. For example in the specialization to plane stress the three in-plane Cartesian components are arranged, following usual FEM conventions, as

$$\mathbf{e} = \begin{bmatrix} e_{xx}(x, y) \\ e_{yy}(x, y) \\ 2e_{xy}(x, y) \end{bmatrix} \tag{2}$$

This strain field is not necessarily compatible (derivable from a continuous displacement field). The source of $\mathbf{e}(\mathbf{x})$ could be experimental, from interpolation of strain gage readings. Or it may be one of the primary fields in strain-assumed finite element formulations. Two related problems, schematized in Figure 2, are studied here:

Strain fitting, or SF problem. Given a continuous displacement field $\mathbf{u}(\mathbf{x})$ and a strain field form $\mathbf{e}(\mathbf{x})$ that contains free parameters, find the parameters that best fit (2). Note that the SF problem is trivial if $\mathbf{e}(\mathbf{x})$ is left completely free since if so $\mathbf{e}(\mathbf{x}) = \mathbf{D}\mathbf{u}(\mathbf{x})$ is obviously the solution.

Displacement fitting, or DF problem. Given $\mathbf{e}(\mathbf{x})$, find an associated displacement field $\mathbf{u}(\mathbf{x})$ in V so that the displacement-derived strain field

$$\mathbf{e}^u(\mathbf{x}) = \mathbf{D}\,\mathbf{u}(\mathbf{x}) \tag{3}$$

matches (1) over V in the sense discussed below. Here $\mathbf{D}$ is the appropriate strain-displacement operator. The fitted displacement field is specified only within a rigid body motion. The symbol $\mathbf{e}^u$ follows the field-dependence notation developed for Parametrized Variational Principles [1–4].

1.2 Applications

Problems DF and SF occur in two application areas.

(I) *Finite Element Technology*. This includes three subareas:

(i) (SF) Development of stiffness equations of finite element structural models based on assumed Cartesian or natural strain fields.

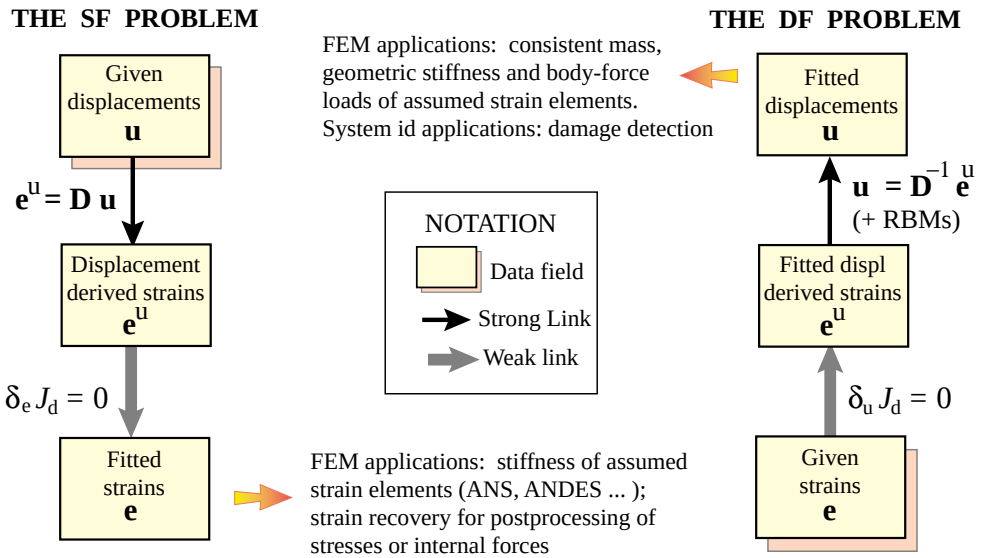

Figure 2. Schematics of the SF (Strain Fitting) and DF (Displacement Fitting) problems.

(ii) (SF) Recovering a strain field from node displacement information, for subsequent post-processing operations on stresses or internal forces.

(iii) (DF) Fitting an internal displacement field to an assumed strain element. This is useful in the computation of consistent masses, body-load node forces and geometric stiffnesses.

(II) *System Identification and Damage Detection*. (DF) A combination of straingage and deflection readings (LVDT, accelerometers) may be available. A displacement field fitted to the former may be used in conjunction with the latter to recover the complete motion over substructures. Details may be found in [5–6].

The present paper focuses on the first application area, namely finite element technology. Selective results may be transported to the second application. The study is confined to linear elasticity. Sections 2 and 3 describe the fitting procedure, Section 4 tools for checking results, and Sections 5 through 8 present examples of use in finite element technology.

2 The Fitting Method

2.1 The Error Functional

The solution of both DF and SF problems is based on the dislocation energy functional

$$J_d[\mathbf{u}, \mathbf{e}] = \tfrac{1}{2} \int_V (\mathbf{e}^u - \mathbf{e})^T \hat{\mathbf{E}} (\mathbf{e}^u - \mathbf{e})\, dV. \tag{4}$$

where $\mathbf{e}^u = \mathbf{D}\mathbf{u}$. Here $\hat{\mathbf{E}}$ is either an *actual* or *fictitious* constitutive matrix, as discussed in §2.4. If actual, $\hat{\mathbf{E}}$ will be simply called $\mathbf{E}$. The solution $\mathbf{u}(\mathbf{x})$ in the DF problem or

$\mathbf{e}(\mathbf{x})$ in the SF problem, is that which minimizes J_d aside from possible displacement rigid-body motions.

For a physical interpretation, consider the first variation with respect to $\mathbf{u}$ in the DF problem. Again following PVP notation denote $\boldsymbol{\sigma}^u = \hat{\mathbf{E}}\mathbf{e}^u = \hat{\mathbf{E}}\mathbf{D}\mathbf{u}$, $\boldsymbol{\sigma}^e = \hat{\mathbf{E}}\mathbf{e}$, $\Delta\boldsymbol{\sigma} = \boldsymbol{\sigma}^u - \boldsymbol{\sigma}^e$ in V, and $\Delta\mathbf{t} \equiv \Delta t_i = \Delta\sigma^e_{ij} n_j$ on S. Then

$$\delta_u J_d = \int_V \Delta\boldsymbol{\sigma}^T\, \delta\mathbf{e}^u\, dV = -\int_V [\mathbf{div}(\Delta\boldsymbol{\sigma}^e)]^T\, \delta\mathbf{u}\, dV + \int_S [\Delta\mathbf{t}]^T\, \delta\mathbf{u}\, dS \qquad (5)$$

If $\hat{\mathbf{E}}$ is an actual constitutive matrix, $\Delta\boldsymbol{\sigma}$ may be viewed as a dislocation stress tensor and $\Delta\mathbf{t}$ as dislocation tractions. It follows that the Euler-Lagrange equation is $\mathbf{div}\,\Delta\boldsymbol{\sigma} = \mathbf{0}$ in V and the natural boundary condition is $\Delta\mathbf{t} = \mathbf{0}$ on S. Physically: the "dislocation stress" $\Delta\boldsymbol{\sigma} = \boldsymbol{\sigma}^u - \boldsymbol{\sigma}^e$, whether real of fictitious, is in self-equilibrium if the variation $\delta_u J_d$ vanishes. The physical interpretation of $\delta_e J_d = 0$ is similar.

2.2 Where Does the Name "Dislocation" Comes From?

It is a long story. To avoid sidetracking the reader, it is enough to mention that dislocation terms were introduced by Friedrichs in the 1930s as a "release path" to go from a functional to its dual, passing through mixed forms along the way. In elasticity such terms look like $\int_V \boldsymbol{\sigma}^T(\mathbf{e}^u - \mathbf{e})\, dV$ or $\int_V \boldsymbol{\sigma}^T(\mathbf{e} - \mathbf{e}^u)\, dV$ when the minimum potential energy functional is treated by Friedrichs' method. Here $\boldsymbol{\sigma}$ is a Lagrange multiplier field with dimension of stress (not necessarily actual stress) while $\mathbf{e}$ and $\mathbf{e}^u$ are incompatible and compatible strain fields, respectively. Physically $\mathbf{e}^u - \mathbf{e}$ represents a continuous field of dislocations, hence the name.

2.3 Real or Fictitious Constitutive Matrix?

For some applications the use of an actual constitutive matrix $\hat{\mathbf{E}} = \mathbf{E}$ in (5) is inconvenient if dependence of the fit on material properties is undesirable. For example, the DF-based construction of consistent mass matrices or body-load force vectors. To avoid the dependence one may simply select $\hat{\mathbf{E}}$ as a diagonal positive-definite weighting matrix, whereby $J_d[\mathbf{u}, \mathbf{e}]$ becomes a weighted least-squares functional. However one should be careful not to damage invariance with respect to the choice of $\{x, y\}$ axes. One choice that preserves such invariance while making $\hat{\mathbf{E}}$ diagonal consists of picking an isotropic material matrix with zero Poisson's ratio ν; in which case the value of the elastic modulus E is irrelevant to the fit and for simplicity we may take $E = 1$.

2.4 Discrete Parameter Fit

In FEM applications, both $\mathbf{e}(\mathbf{x})$ and $\mathbf{u}(\mathbf{x})$ are linear functions of a finite number of free parameters g_i and q_i, respectively. The N_g strain parameters g_i are collected in a vector $\mathbf{g}$ while the N_q displacement generalized coordinates q_i are collected in a vector $\mathbf{q}$. Usually $N_g < N_q$ since the latter often includes rigid body modes as discussed in §2.5. The matrix form representation is

$$\mathbf{e}(\mathbf{x}) = \mathbf{B}_e(\mathbf{x})\,\mathbf{g}, \qquad \mathbf{e}^u(\mathbf{x}) = \mathbf{B}_u(\mathbf{x})\,\mathbf{q} = \mathbf{D}\,\mathbf{N}_u(\mathbf{x})\,\mathbf{q}. \qquad (6)$$

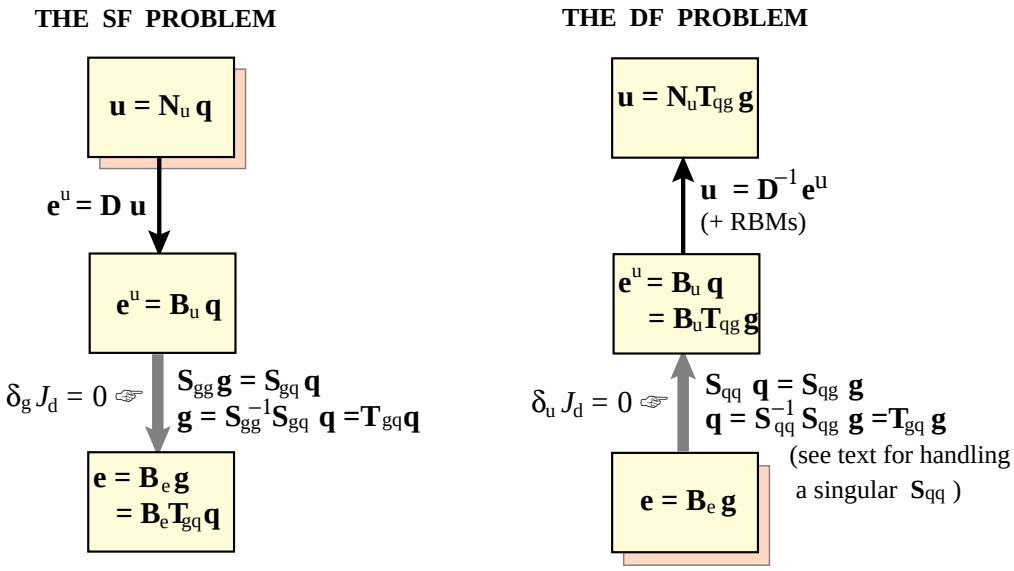

Figure 3. Discrete parameter fit summary.

where matrices $\mathbf{B}_e$, $\mathbf{B}_u$ and $\mathbf{N}_u$ depend on the position coordinates. Matrix $\mathbf{N}_u$ contains the usual shape functions if the q_i are node displacement; else it is built with generalized shape functions.

The fitting procedure based on (4) becomes a Ritz analysis. Substitution of (6) into (4) generates the quadratic form

$$J_d(\mathbf{g},\mathbf{q}) = \tfrac{1}{2}\mathbf{g}^T\mathbf{S}_{gg}\mathbf{g} - \tfrac{1}{2}\mathbf{g}^T\mathbf{S}_{gq}\mathbf{u} - \tfrac{1}{2}\mathbf{u}^T\mathbf{S}_{qg}\mathbf{g} + \tfrac{1}{2}\mathbf{q}^T\mathbf{S}_{qq}\mathbf{q}, \tag{7}$$

where

$$\mathbf{S}_{gg} = \int_V \mathbf{B}_e^T\hat{\mathbf{E}}\mathbf{B}\,dV,\;\; \mathbf{S}_{gq} = \int_V \mathbf{B}_e^T\hat{\mathbf{E}}\mathbf{B}_u\,dV,\;\; \mathbf{S}_{qg} = \mathbf{S}_{gq}^T,\;\; \mathbf{S}_{qq} = \int_V \mathbf{B}_u^T\hat{\mathbf{E}}\mathbf{B}_u\,dV. \tag{8}$$

These matrices have dimension of stiffness but are not necessarily physical because $\hat{\mathbf{E}}$ may be fictitious. Matrices $\mathbf{S}_{gg}$ and $\mathbf{S}_{qq}$ are square and symmetric whereas $\mathbf{S}_{gq}$ and $\mathbf{S}_{qg}$ are usually rectangular.

For problem SF, set $\delta_g\, J_d = (\partial J_d/\partial\mathbf{g})^T\delta\,\mathbf{g} = 0$ and solve for $\mathbf{g}$ in terms of $\mathbf{q}$:

$$\mathbf{g} = \mathbf{S}_{gg}^{-1}\,\mathbf{S}_{gq}\,\mathbf{q} = \mathbf{T}_{gq}\,\mathbf{q}. \tag{9}$$

This is a well posed problem if the strain patterns associated with the g_i are linearly independent because if so $\mathbf{B}_e$ has full rank and $\mathbf{S}_{gg}$ is positive definite.

For problem DF, set $\delta_q\, J = (\partial J_d/\partial\mathbf{q})^T\delta\,\mathbf{q} = 0$ and solve for $\mathbf{q}$ in terms of $\mathbf{g}$:

$$\mathbf{q} = \mathbf{S}_{qq}^{-1}\,\mathbf{S}_{qg}\,\mathbf{g} = \mathbf{T}_{qg}\,\mathbf{g}. \tag{10}$$

This problem is not generally well posed, as discussed next.

2.5 Treating Rigid Body Modes in the DF Problem

A problem arises with (10) if the body is unconstrained: $\mathbf{S}_{qq}$ is singular on account of the presence of $N_r > 0$ rigid body modes (RBMs). Two cases may be distinguished.

Case 1. The RBMs are explicitly isolated in the set $\mathbf{q}$ so that $\mathbf{q} = [\ \mathbf{q}_r\ \ \mathbf{q}_d\ ]$, where $\mathbf{q}_r$ are RBM amplitudes and $\mathbf{q}_d$ amplitudes of deformational displacement modes. This leads to the obvious splitting

$$\mathbf{u}(\mathbf{x}) = \mathbf{u}_r(\mathbf{x}) + \mathbf{u}_d(\mathbf{x}) = \mathbf{N}_r\,\mathbf{q}_r + \mathbf{N}_d\,\mathbf{q}_d, \qquad \mathbf{e}^u = \mathbf{D}\mathbf{N}_d\mathbf{q}_d = \mathbf{B}_u\mathbf{q}_d, \tag{11}$$

since $\mathbf{D}\mathbf{N}_r = \mathbf{0}$. Then (10) is executed with $\mathbf{q} \to \mathbf{q}_d$, that is, carrying along only the deformational displacement modes:

$$\mathbf{q}_d = \mathbf{S}_{qq}^{-1}\mathbf{S}_{qg}\,\mathbf{g} = \mathbf{T}_{qg}\mathbf{g}. \tag{12}$$

and $\mathbf{q}_d$ is augmented with the RMS amplitudes to form $\mathbf{q}$. This technique is related to the Free Formulation discussed in §4.2.

Case 2. The RBMs are enmeshed in $\mathbf{q}$. This is the case where the q_i are physical node displacements. A splitting into $\mathbf{q} = [\ \mathbf{q}_r\ \ \mathbf{q}_d\ ]$ is possible using the machinery of the Free Formulation [7], but it is often simpler to proceed as follows. As first step, form a full-rank $N_q \times N_r$ matrix $\mathbf{R}$ that fully spans the RBM motions as

$$\mathbf{u}_r = \mathbf{R}\mathbf{a}, \tag{13}$$

where $\mathbf{a}$ denotes the N_r RBM amplitudes. The N_r columns of $\mathbf{R}$ represent RBM motions in the $\mathbf{q}$ coordinates. (That is, $\mathbf{R}$ is a basis for the null space of $\mathbf{B}_u$.) Next, orthonormalize $\mathbf{R}$ so that $\mathbf{R}^T\mathbf{R} = \mathbf{I}_r$, where $\mathbf{I}_r$ is the identity matrix of order N_r. Form the orthogonal projector $\mathbf{P} = \mathbf{I}_q - \mathbf{R}\mathbf{R}^T$, where $\mathbf{I}_q$ is the identity matrix of order N_q. Finally, replace (10) by

$$\mathbf{q} = \mathbf{F}_{qq}\mathbf{S}_{qg}\,\mathbf{g} = \mathbf{T}_{qg}\,\mathbf{g}, \quad \text{with} \quad \mathbf{F}_{qq} = \mathbf{S}_{qq}^{+} = \mathbf{P}(\mathbf{S}_{qq} + \mathbf{R}\mathbf{R}^T)^{-1}. \tag{14}$$

Here $\mathbf{F}_{qq}$ is the free-free flexibility [8,9] associated with $\mathbf{S}_{qq}$. Mathematically, $\mathbf{F}_{qq}$ and $\mathbf{S}_{qq}$ are the Moore-Penrose generalized inverses of each other.

2.6 Approximation Sequences

In the DF problem, field $\mathbf{e}(\mathbf{x})$ is often a polynomial in the space coordinates $\mathbf{x}$. In that case the displacement Ritz basis defined by $\mathbf{N}_q$ can be taken to be the complete span of polynomials of appropriate order. If the field $\mathbf{e}$ *is compatible*, from a certain basis onward we obtain the exact displacement fit $\mathbf{e} = \mathbf{e}^u = \mathbf{D}\mathbf{u}$, which is independent of $\mathbf{E}$, and $J_d = 0$. If $\mathbf{e}$ is polynomial but incompatible, from a certain basis onward the fitted solution may not improve in the sense that J_d attains a minimum and stays there. However this approximate fit will generally depend on the choice for $\mathbf{E}$; cf. §2.4.

A similar phenomenon may occur in the SF problem. However in this case the gaged field is typically kept deliberately to be of lower order than $\mathbf{e}^u$ to get around de Veubeke's limitation principle.

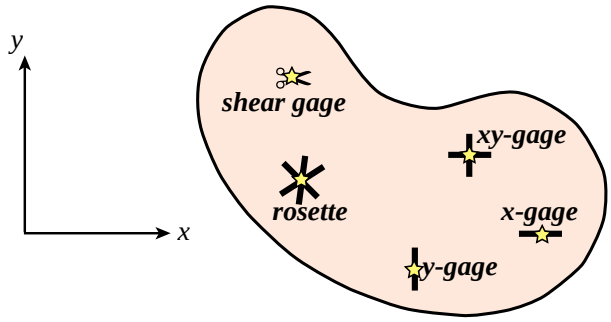

Figure 4. Straingage visualization over a 2D body. In FEM work straingages are often collocated at Barlow points.

2.7 Straingage Visualization

If (1) is a gaged field, collocated strain values are pictured by *straingage* symbols. These are used for visualization convenience and do not imply an actual experimental setup. Figure 4 illustrates symbols used to identify straingage locations and directions on a 2D body. For example, an x-gage measures the extensional strain e_{xx} at the star point, whereas an xy-shear gage that measures $2e_{xy}$ is pictured as a scissor (note that such devices are not experimentally realizable). An xy-gage measures e_{xx} and e_{yy} at the same point. A 2D rosette measures the 3 extensional components in 3 directions, from which the Cartesian components (2) may be computed. Rosette arrangements are frequently found when using natural strains in finite element work. As the examples in Sections 4ff show, straingages are usually placed at the so-called Barlow points [10].

2.8 The Stress-Displacement Fitting Problem

The foregoing method can be used with little change for fitting displacements to stress fields or vice-versa. It is only necessary to replace $\mathbf{e}$ by $\mathbf{e}^\sigma = \mathbf{E}^{-1}\boldsymbol{\sigma}$, where $\boldsymbol{\sigma}$ is the stress field under consideration, and the dislocation functional becomes

$$J_d[\mathbf{u},\boldsymbol{\sigma}] = \tfrac{1}{2}\int_V (\mathbf{e}^u - \mathbf{E}^{-1}\boldsymbol{\sigma})^T \hat{\mathbf{E}}(\mathbf{e}^u - \mathbf{E}^{-1}\boldsymbol{\sigma})\, dV. \tag{15}$$

with a obvious reduction if $\mathbf{E} = \hat{\mathbf{E}}$. This is useful in the construction of elements based on the Hellinger-Reissner principle.

3 Energy Orthogonal Hierarchical Fitting

When dealing with general multidimensional geometries it is often convenient to proceed in stages using an energy orthogonal (EO) hierarchical approach. For example, suppose that $\mathbf{e}(\mathbf{x})$ is *linear* in the position coordinates $\mathbf{x}$. Decompose $\mathbf{e}$ into a mean strain $\bar{\mathbf{e}}$ constant over V, and an EO deviatoric strain $\mathbf{e}_d$:

$$\mathbf{e} = \bar{\mathbf{e}} + \mathbf{e}_d, \quad \text{subject to} \quad \int_V \delta\bar{\mathbf{e}}^T\, \mathbf{E}\, \mathbf{e}_d\, dV = 0 \quad \text{or} \quad \int_V \mathbf{E}\, \mathbf{e}_d\, dV = \mathbf{0}. \tag{16}$$

For a body with constant $\mathbf{E}$ the EO condition reduces to $\int_V \mathbf{e}_d\, dV = \mathbf{0}$, which for linear $\mathbf{e}$ is satisfied if

$$\bar{\mathbf{e}} = \mathbf{e}(\mathbf{x}_C) \tag{17}$$

where $\mathbf{x}_C$ is the body centroid position. For a nonuniform body, or a $\mathbf{e}$ nonlinear in the position coordinates (as in axisymmetric problems) the rule (17) is not valid.

Since a uniform strain field is always compatible, $\bar{\mathbf{e}}$ can be exactly fitted, within a rigid body motion, by a linearly varying displacement $\bar{\mathbf{u}}$ such that $\bar{\mathbf{e}} = \mathbf{D}\bar{\mathbf{u}}$. Split $\mathbf{u} = \bar{\mathbf{u}} + \mathbf{u}_d$. The dislocation functional reduces to

$$J_d[\mathbf{u}_d] = \tfrac{1}{2}\int_V (\mathbf{D}\mathbf{u}_d - \mathbf{e}_d)^T \mathbf{E}\,(\mathbf{D}\mathbf{u}_d - \mathbf{e}_d)\, dV, \tag{18}$$

and the problem is reduced to minimizing J_d to find the deviatoric displacement $\mathbf{u}_d$, which is purely deformational. This hierarchical process can be applied over more stages if the variation of $\mathbf{e}$ is superlinear.

Where does the EO condition in (16) come from? From the auxiliary problem of finding the uniform strain that best fits the given strain, using the error functional

$$\bar{J}[\bar{\mathbf{e}}] = \tfrac{1}{2}\int_V (\bar{\mathbf{e}} - \mathbf{e})^T \mathbf{E}(\bar{\mathbf{e}} - \mathbf{e})\, dV. \tag{19}$$

Vanishing of the first variation of $\bar{J}$ gives the second of (16).

4 Fitting Decisions

In two and three dimensions the SF problem may be ambiguous even if the number of g_i parameters is fixed. Decisions may have to be taken on various matters, notably the following two.

High order strain patterns. The assumption $\mathbf{e} = \mathbf{B}_e\mathbf{g}$ should have enough approximation power to represent uniform strain states. Decisions beyond that threshold may have to be taken if the higher order variation is incomplete.

Quadrature rule. If the body or element geometry is complicated the integrals (8) must be done numerically. Which brings decisions such as: (i) which quadrature rule is used, (ii) whether the same rule is chosen for all integrals, and (iii) whether an exact or approximate Jacobian determinant is used in $\mathbf{B}_u$.

If the fitting is done for stress postprocessing and visualization one may afford to be cavalier and chose any convenient scheme. But for element stiffness construction seemingly innocuous design changes may produce an element that does not work. The patch test comes to the rescue to keep the process on tarck. But using *a posteriori* patch tests is often futile. Even if one runs 10^{30} multielement patch tests over the next billion years, there is no guarantee that test number $10^{30}+1$ will be passed. And failed tests may give no clue where the problem lies. It is preferably to work with a test that works *a priori* at the element level.

4.1 IET and the Free Formulation

The Individual Element Test (IET) of Bergan and Hanssen [11] provides sufficient conditions for an element to pass the patch test without having to run all possible multielement combinations. The price paid is that the conditions are stronger than necessary in some cases. The IET is also constructive. In conjunction with the Free Formulation [7] and derived techniques it provide element design rules that can be applied with symbolic computations. We describe here rules useful for testing fitted strain fields.

In the framework of the Free Formulation (FF), the key idea is that element node displacement vector $\mathbf{u}$ can be modally decomposed as $\mathbf{u} = \mathbf{u}_r + \mathbf{u}_c + \mathbf{u}_h$, which are associated with rigid body motions, constant strain states and higher order modes, respectively. The expansion over the element is

$$\mathbf{u} = \mathbf{G}_r\mathbf{q}_r + \mathbf{G}_c\mathbf{q}_c + \mathbf{G}_h\mathbf{q}_h = [\,\mathbf{G}_r \quad \mathbf{G}_c \quad \mathbf{G}_h\,]\begin{bmatrix}\mathbf{q}_r\\ \mathbf{q}_c\\ \mathbf{q}_h\end{bmatrix} = \mathbf{G}\mathbf{q}. \tag{20}$$

where $\mathbf{q}_r$, $\mathbf{q}_c$ and $qbold_h$ are generalize coordinate amplitudes and the $\mathbf{G} = \mathbf{G}(\mathbf{x})$'s are displacement patterns. The higher order patterns $\mathbf{G}_h$ are not necessarily conforming, hence the "Free" qualifier in the method name. The dimension of $\mathbf{u}$ and $\mathbf{q}$ must be the same and the square matrix $\mathbf{g}$ must have full rank. The displacement derived strains are

$$\mathbf{e}^u = \mathbf{D}\mathbf{G}\mathbf{q} = \mathbf{D}\mathbf{G}_r\mathbf{q}_r + \mathbf{D}\mathbf{G}_c\mathbf{q}_c + \mathbf{D}\mathbf{G}_h\mathbf{q}_h = \mathbf{B}^q_c\mathbf{q}_c + \mathbf{B}^q_h\mathbf{q}_h = \mathbf{e}^q_c + \mathbf{e}^q_h. \tag{21}$$

since $\mathbf{D}\mathbf{N}_r = \mathbf{0}$. Since $\mathbf{G}$ is required to be nonsingular, inversion of (20) yields

$$\mathbf{q} = \mathbf{G}^{-1}\mathbf{u} = \mathbf{H}\mathbf{u} = [\,\mathbf{H}_r \quad \mathbf{H}_c \quad \mathbf{H}_h\,]\begin{bmatrix}\mathbf{u}_r\\ \mathbf{u}_c\\ \mathbf{u}_h\end{bmatrix} \tag{22}$$

One of the two IET conditions are the orthogonality constraints $\mathbf{B}_h\mathbf{u}_r = \mathbf{0}$, $\mathbf{B}_h\mathbf{u}_c = \mathbf{0}$ which express that rigid body motions and constant strain states must not produce any higher order starins. Since $\mathbf{u}_{rc} = \mathbf{G}_{rc}\mathbf{q}$ and $\mathbf{q}$ is arbitrary, the appropriate matrix test is

$$\mathbf{B}^u_h\mathbf{G}_r = \mathbf{0}, \qquad \mathbf{B}^u_h\mathbf{G}_c = \mathbf{0}. \tag{23}$$

Bergan [12] called this an *energy orthogonality* condition.

4.2 Strain Elements and the IET

In assumed strain elements based on a fitted strain field $\mathbf{e} = \mathbf{B}^e\mathbf{g}$ the physical stiffness matrix is given by

$$\mathbf{K} = \mathbf{T}^T_{qg}\mathbf{K}_{gg}\mathbf{T}_{gq}, \quad \mathbf{K}_{gg} = \int_V (\mathbf{B}^e)^T\mathbf{E}_m\mathbf{B}^e\,dV. \tag{24}$$

where $\mathbf{T}_{gq}$ is constructed as discussed in §2.4. Note that $\mathbf{K}_{gg}$ has the same expression as $\mathbf{S}_{gg}$ in (2) but here $\mathbf{E}_m$ is the actual constitutive matrix whereas $\mathbf{E}$ might be fictitious. *There is no a priori guarantee that* (24) *will pass the patch test*. Generally it won't.

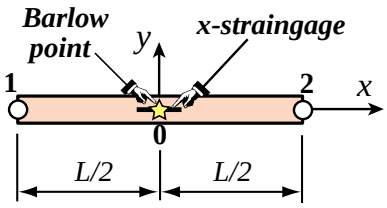

Figure 5. Bar with uniform strain distribution.

To guarantee *a priori* satisfaction the FF energy orthogonality conditions (23) can be transcribed to strain elements. It is necessary to decompose the fitted strain into mean and higher order part:

$$\mathbf{e} = \bar{\mathbf{e}} + \mathbf{B}_h^e \mathbf{g} \tag{25}$$

and enforce

$$\mathbf{B}_h \mathbf{G}_r = \mathbf{0}, \quad \mathbf{B}_h \mathbf{G}_c = \mathbf{0} \tag{26}$$

One way to achieve this result automatically is to chose the higher order fitted strains to be deviatoric in the sense discussed in §2.4. This is the method of Assumed Natural DEviatoric Strains, or ANDES [13,14].

5 DF: Bar Element

A free-free 2-node bar element of elastic modulus E and uniform cross section area A extends from $x = -\frac{1}{2}L$ (node 1) to $x = \frac{1}{2}L$ (node 2), as shown in Figure 5. Only axial motions are considered. A straingage at the midpoint $x = 0$ (the only Barlow point) registers the strain e_0. This is extended over the whole bar so the given strain is $e = e_0$. Find a matching axial displacement $u(x)$.

The error functional is

$$J[u] = \tfrac{1}{2}\int_{-L/2}^{L/2} EA(e^u - e)^2\, dx = \tfrac{1}{2}\int_{-L/2}^{L/2} EA\left(\frac{du}{dx} - e_0\right)^2 dx \tag{27}$$

Assuming $u(x) = a_0 + a_1 x$ we obtain the Ritz solution $a_1 = e_0$ whereas a_0 is arbitrary. Hence $u(x) = u_R + u_d$, in which $u_R = a_0 = \alpha_1$ is identified as the only rigid body motion and $u_d = e_0 x$ is the deformational motion. Evaluation at the nodes yields

$$\begin{bmatrix} u_1 \\ u_2 \end{bmatrix} = \begin{bmatrix} 1 \\ 1 \end{bmatrix} \alpha_1 + \tfrac{1}{2}L \begin{bmatrix} -1 \\ 1 \end{bmatrix} e_0 = \mathbf{R}\boldsymbol{\alpha} + \mathbf{Q}\mathbf{g}. \tag{28}$$

Since the strain field is compatible the fit is exact and both material and area properties drop out. Note that $\mathbf{Q}$ is orthogonal to $\mathbf{R}$. The result (28) is well known.

6 DF: Beam Element with Hermitian Basis

A free-free, 2-node Bernoulli-Euler plane-beam element of elastic modulus E and uniform moment of inertia I extends from $x = -\frac{1}{2}L$ (node 1) to $x = \frac{1}{2}L$ (node 2) as shown in Figure 6. Only transverse motions are considered. Two straingage pairs are placed at the Barlow points $x = \pm L/(2\sqrt{3})$, which are also the sample points of the 2-point Gauss rule. Curvatures κ_1 and κ_2 are measured there. In an experimental setting these would be obtained by subtracting top and bottom gage readings, and dividing by the height. The linear curvature variation extrapolated from these measurements over the entire beam is

$$\kappa(x) = \tfrac{1}{2}(\kappa_1 + \kappa_2) + \sqrt{3}(\kappa_1 - \kappa_2)\frac{x}{L} \tag{29}$$

The error functional is

$$J[u] = \tfrac{1}{2}\int_{-L/2}^{L/2} EI\,(\kappa^u - \kappa)^2\,dx = \tfrac{1}{2}\int_{-L/2}^{L/2} EI\left(\frac{d^2w}{dx^2} - \kappa\right)^2 dx \tag{30}$$

where w is the transverse beam displacement. Assume the trial cubic displacement field:

$$w = q_0 + q_1\frac{x}{L} + q_2\frac{x^2}{L^2} + q_3\frac{x^3}{L^3} \tag{31}$$

in which all q_i coefficients have dimension of length. Substituting (29) and (31) into (30) and performing the minimization yields $q_2 = \frac{1}{4}(\kappa_1 + \kappa_2)L$ and $q_3 = \frac{1}{2}(\kappa_1 - \kappa_2)L^2/\sqrt{3}$ whereas q_0 and q_1 are arbitrary. Consequently the fitted displacement is

$$w = \alpha_1 + \alpha_2\frac{x}{L} + \frac{1}{4}(\kappa_1 + \kappa_2)x^2 + \frac{1}{2\sqrt{3}L}(\kappa_1 - \kappa_2)x^3 \tag{32}$$

in which q_0 and q_1 have been renamed a_1 and a_2 respectively, because they can be directly identified as rigid body mode amplitudes. Evaluating (32) at the end nodes in terms of the standard 4 degrees of freedom $w_1 = w(-L/2)$, $\theta_1 = w_x(-L/2)$, $w_2 = w(L/2)$ and $\theta_2 = w_x(L/2)$ yields the matrix relations

$$\begin{bmatrix} w_1 \\ \theta_1 \\ w_2 \\ \theta_2 \end{bmatrix} = \begin{bmatrix} 1 & -1/2 \\ 0 & -1/L \\ 1 & 1/2 \\ 0 & 1/L \end{bmatrix}\begin{bmatrix} \alpha_1 \\ \alpha_2 \end{bmatrix} + \frac{L^2}{48}\begin{bmatrix} -\sqrt{3}+3 & \sqrt{3}+3 \\ 6(\sqrt{3}-2) & -6(\sqrt{3}+2) \\ \sqrt{3}+3 & -\sqrt{3}+3 \\ 6(\sqrt{3}+2) & -6(\sqrt{3}-2) \end{bmatrix}\begin{bmatrix} \kappa_1 \\ \kappa_2 \end{bmatrix} = \mathbf{R}\boldsymbol{\alpha} + \mathbf{Q}\boldsymbol{\kappa}. \tag{33}$$

As a check, we take the well known stiffness matrix of the cubic Hermitian C^1 beam and perform a congruential transformation with the stacked $\mathbf{R}$ and $\mathbf{Q}$ to form a generalized stiffness matrix in terms of α_1, α_2, κ_1 and κ_2:

$$\begin{bmatrix} \mathbf{R}^T \\ \mathbf{Q}^T \end{bmatrix}\frac{EI}{L^3}\begin{bmatrix} 12 & 6L & -12 & 6L \\ 6L & 4L^2 & -6L & 2L^2 \\ -12 & -6L & 12 & -6L \\ 6L & 2L^2 & -6L & 4L^2 \end{bmatrix}[\,\mathbf{R} \quad \mathbf{Q}\,] = EI\,L\begin{bmatrix} 0 & 0 & 0 & 0 \\ 0 & 0 & 0 & 0 \\ 0 & 0 & \frac{1}{2} & 0 \\ 0 & 0 & 0 & \frac{1}{2} \end{bmatrix} \tag{34}$$

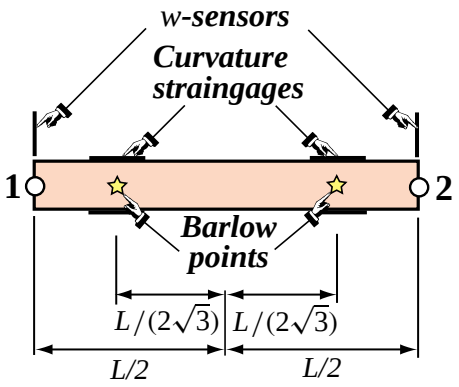

Figure 6. Plane beam element with given strain distribution.

Because the curvature gages have been placed at the Barlow points, the generalized stiffness matrix (34) is diagonal. The result (32) also answers the question: what is the best quadratic curvature fit? Just drop the x^3 term.

Relations (32) and (33) have applications in measurement of beam member motions. Beam strains (and hence curvatures) as well as translational motions can be easily and accurately measured with straingages and LVDT sensors, respectively, whereas rotations are not. These relations suggest placing straingages at the two Barlow points and translational sensors at the end points to record $\kappa_1(t)$, $\kappa_2(t)$, $w_1(t)$ and $w_2(t)$ as function of time t. From the latter one recovers $a_1(t) = \frac{1}{2}(w_1 + w_2)$, $a_2(t) = (w_1 - w_2)/L$ and hence the complete history $w(x,t)$ from (32). Derived quantities such as kinetic energy can be then readily computed.

7 DF: Beam with RBM-Orthogonal Deformational Basis

In some applications, such as damage detection, it is convenient to have the deformational basis matrix **Q** be orthogonal to the rigid-body basis matrix **R**. This can always be done *a posteriori* by a Gram-Schmidt orthogonalization process applied to **Q**. For the beam example this can be done *a priori* by assuming the following Ritz trial expansion:

$$w = q_0 + q_1\frac{x}{L} + q_2\left(\frac{x^2}{L^2} - \frac{1}{4}\right) + q_3\left(\frac{x^3}{L^3} - \frac{12+L^2}{4+L^2}\frac{x}{4L}\right) \tag{35}$$

in which the two deformation modes are modified by rigid body modes. Note that the modification of the last function is not dimensionally homogeneous. Substituting into the error functional and performing the minimization yields the same values of a_2 and a_3 and consequently the fitted displacement is

$$w = a_1 + a_2\frac{x}{L} + \frac{L^2}{4}(\kappa_1+\kappa_2)\left(\frac{x^2}{L^2} - \frac{1}{4}\right) + \frac{L^2}{2\sqrt{3}}(\kappa_1-\kappa_2)\left(\frac{x^3}{L^3} - \frac{(12+L^2)}{(4+L^2)}\frac{x}{4L}\right) \tag{36}$$

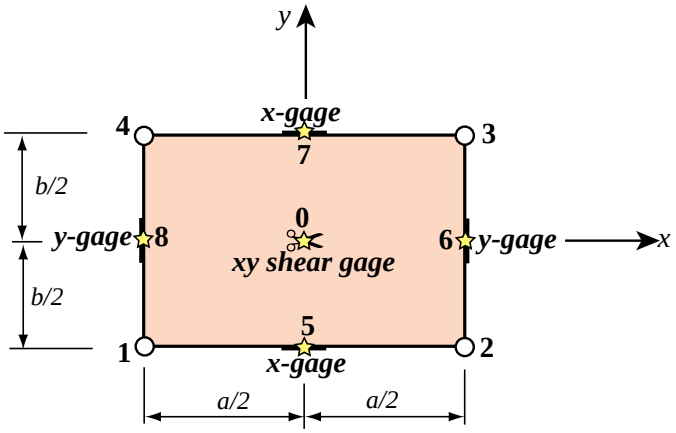

Figure 7. Rectangular 4-node plane stress element with given strain distribution.

Evaluating this at the nodes provides the same **R** as in (33) but a different **Q** which is orthogonal to **R**, i.e. $\mathbf{Q}^T\mathbf{R} = \mathbf{0}$. Transformation to the generalized stiffness matrix yields the same result as (34).

Further development and applications of these interpolations in the context of plane beam templates for structural dynamics are studied in [15,16].

8 DF: 4-Node Rectangular Panel Element

We consider a free-free, 4-corner-node plane stress rectangular element of side dimensions a and b along x and y, respectively. See Figure 7. The element has constant thickness h and constitutive matrix **E**. The coordinates of nodes 1, 2, 3 and 4 are $(-\frac{1}{2}a, -\frac{1}{2}b)$, $(\frac{1}{2}a, -\frac{1}{2}b)$, $(\frac{1}{2}a, \frac{1}{2}b)$, and $(-\frac{1}{2}a, \frac{1}{2}b)$, respectively. The four midpoints between 1-2, 2-3, 3-4 and 4-1 are labeled 5, 6, 7 and 8, respectively. The centroid $x = y = 0$ is labelled 0. Five straingages are placed over the element: two extensional gages to measure e_{xx} at midpoints 5 and 7, two extensional gages to measure e_{yy} at midpoints 6 and 8, and one shear rosette to measure e_{xy} at the centroid 0. The gaged strain field over the element is assumed to be

$$\mathbf{e}(x,y) = \begin{bmatrix} e_{xx}(x,y) \\ e_{yy}(x,y) \\ 2e_{xy}(x,y) \end{bmatrix} = \begin{bmatrix} \frac{1}{2}(1-y/b)e_{xx5} + \frac{1}{2}(1+y/b)e_{xx7} \\ \frac{1}{2}(1+x/a)e_{yy6} + \frac{1}{2}(1-x/a)e_{yy8} \\ 2e_{xy0} \end{bmatrix} \tag{37}$$

The displacement field to be fitted is that of the bilinear element:

$$u_x = a_{00} + a_{10}x + a_{01}y + a_{11}xy, \quad u_y = b_{00} + b_{10}x + b_{01}y + b_{11}xy. \tag{38}$$

so that

$$\mathbf{e}^u = \begin{bmatrix} a_{10} + a_{11}y \\ b_{01} + b_{11}x \\ a_{01} + a_{11}x + b_{10} + b_{11}y \end{bmatrix} \tag{39}$$

Although (38) is compatible, (39) lacks approximation power to fit it exactly, and a dislocation field appears. Consequently the fit will depend on the material properties.

The error functional is

$$J = \tfrac{1}{2}\int_{-a/2}^{a/2}\int_{-b/2}^{b/2} (\mathbf{e}^u - \mathbf{e})^T\, \mathbf{E}\, (\mathbf{e}^u - \mathbf{e})\, dx\, dy. \tag{40}$$

For isotropic material with Poisson's ratio ν, the best fit is

$$\begin{aligned} u_x &= \alpha_1 + \tfrac{1}{2}(e_{xx5} + e_{xx7})x + (-\alpha_3 + e_{xy0})y + \frac{b}{2b^2 + a^2 - a^2\nu}(e_{xx7} - e_{xx5})xy, \\ u_y &= \alpha_2 + (\alpha_3 + e_{xy0})x + \tfrac{1}{2}(e_{yy6} + e_{yy8})y + \frac{a}{2a^2 + b^2 - b^2\nu}(e_{yy6} - e_{yy8})xy, \end{aligned} \tag{41}$$

in which $\alpha_1 = a_{00}$, $\alpha_2 = b_{00}$ and $\alpha_3 = \frac{1}{2}(b_{10} - a_{01})$ are the three rigid body mode amplitudes. Evaluation at the nodes gives

$$\begin{aligned} \begin{bmatrix} u_{x1} \\ u_{y2} \\ u_{x2} \\ u_{y2} \\ u_{x3} \\ u_{y3} \\ u_{x4} \\ u_{y4} \end{bmatrix} &= \begin{bmatrix} 1 & 0 & \frac{1}{2}b \\ 0 & 1 & -\frac{1}{2}a \\ 1 & 0 & \frac{1}{2}b \\ 0 & 1 & \frac{1}{2}a \\ 1 & 0 & -\frac{1}{2}b \\ 0 & 1 & \frac{1}{2}a \\ 1 & 0 & -\frac{1}{2}b \\ 0 & 1 & -\frac{1}{2}a \end{bmatrix} \begin{bmatrix} \alpha_1 \\ \alpha_2 \\ \alpha_3 \end{bmatrix} + \tfrac{1}{4} \begin{bmatrix} -ar_3 & -ar_4 & 0 & 0 & -2b \\ 0 & 0 & -br_2 & -br_1 & -2a \\ ar_3 & ar_4 & 0 & 0 & -2b \\ 0 & 0 & -br_1 & -br_2 & 2a \\ ar_4 & ar_3 & 0 & 0 & 2b \\ 0 & 0 & br_1 & br_2 & 2a \\ -ar_4 & -ar_3 & 0 & 0 & 2b \\ 0 & 0 & br_2 & br_1 & -2a \end{bmatrix} \begin{bmatrix} e_{xx5} \\ e_{xx7} \\ e_{yy6} \\ e_{yy8} \\ e_{xy0} \end{bmatrix} \\ &= \mathbf{R}\boldsymbol{\alpha} + \mathbf{Q}\mathbf{g}, \end{aligned} \tag{42}$$

in which $r_1 = 1+\chi_a, r_2 = 1-\chi_a, r_3 = 1+\chi_b, r_4 = 1-\chi_b$, $\chi_a = a^2/(2a^2+b^2-b^2\nu)$ and $\chi_b = b^2/(2b^2 + a^2 - a^2\nu)$. Inversion of $[\mathbf{R} \quad \mathbf{Q}]$ gives RBM amplitudes and straingage readings in terms of node displacements. This can be used to obtain an assumed-strain plane stress element.

An interesting application of (41) is the construction of a consistent mass matrix in terms of $\boldsymbol{\alpha}$ and $\mathbf{g}$. The result is

$$\mathbf{M}_g = \frac{\rho A h}{48} \begin{bmatrix} 48 & 0 & 0 & 0 & 0 & 0 & 0 & 0 \\ 0 & 48 & 0 & 0 & 0 & 0 & 0 & 0 \\ 0 & 0 & a^2+b^2 & 0 & 0 & 0 & 0 & 2(a^2-b^2) \\ 0 & 0 & 0 & M_{44} & M_{45} & 0 & 0 & 0 \\ 0 & 0 & 0 & M_{45} & M_{55} & 0 & 0 & 0 \\ 0 & 0 & 0 & 0 & 0 & M_{66} & M_{67} & 0 \\ 0 & 0 & 0 & 0 & 0 & M_{67} & M_{77} & 0 \\ 0 & 0 & 2(a^2-b^2) & 0 & 0 & 0 & 0 & 4(a^2+b^2) \end{bmatrix} \tag{43}$$

where $A = ab$, $M_{44} = M_{55} = a^2 + \frac{1}{3}a^2b^4/(2b^2+a^2-a^2\nu)^2$, $M_{45} = a^2 - \frac{1}{3}a^2b^4/(2b^2 + a^2 - a^2\nu)^2$, etc. This may be congruentially transformed by $\mathbf{T} = [\mathbf{R} \quad \mathbf{Q}]^{-1}$ to get a

consistent mass matrix $\mathbf{T}$ in terms of the physical node displacements. For $\nu = 0$ that inverse is

$$\begin{bmatrix}
\frac{1}{4} & 0 & \frac{1}{4} & 0 & \frac{1}{4} & 0 & \frac{1}{4} & 0 \\
0 & \frac{1}{4} & 0 & \frac{1}{4} & 0 & \frac{1}{4} & 0 & \frac{1}{4} \\
\frac{1}{4b} & -\frac{1}{4a} & \frac{1}{4b} & \frac{1}{4a} & -\frac{1}{4b} & \frac{1}{4a} & -\frac{1}{4b} & -\frac{1}{4a} \\
-\frac{3}{2a}-\frac{a}{2b^2} & 0 & \frac{3}{2a}+\frac{a}{2b^2} & 0 & \frac{-a^2-b^2}{2ab^2} & 0 & \frac{1}{2a}+\frac{a}{2b^2} & 0 \\
\frac{1}{2a}+\frac{a}{2b^2} & 0 & \frac{-a^2-b^2}{2ab^2} & 0 & \frac{3}{2a}+\frac{a}{2b^2} & 0 & -\frac{3}{2a}-\frac{a}{2b^2} & 0 \\
0 & \frac{1}{2b}+\frac{b}{2a^2} & 0 & -\frac{3}{2b}-\frac{b}{2a^2} & 0 & \frac{3}{2b}+\frac{b}{2a^2} & 0 & \frac{-a^2-b^2}{2a^2b} \\
0 & -\frac{3}{2b}-\frac{b}{2a^2} & 0 & \frac{1}{2b}+\frac{b}{2a^2} & 0 & \frac{-a^2-b^2}{2a^2b} & 0 & \frac{3}{2b}+\frac{b}{2a^2} \\
-\frac{1}{4b} & -\frac{1}{4a} & -\frac{1}{4b} & \frac{1}{4a} & \frac{1}{4b} & \frac{1}{4a} & \frac{1}{4b} & -\frac{1}{4a}
\end{bmatrix} \tag{44}$$

The mass matrix in terms of node displacements is $\mathbf{M} = \mathbf{T}^T \mathbf{M}_g \mathbf{T}$.

9 Conclusion

The Strain Fitting procedure is being presently used in the derivation of optimal stiffness of quadrilateral and solid-shell elements by ANDES methods. Examples to this effect are omitted on account of length limitations.

Acknowledgement

Preparation of the present paper has been supported by Sandia National Laboratories under the Finite Elements for Salinas contract award.

References

[1] C. A. Felippa and C. Militello, "*Developments in Variational Methods for High Performance Plate and Shell Elements*," in Analytical and Computational Models for Shells, CED Vol. 3, ed. by A. K. Noor, T. Belytschko and J. C. Simo, ASME, New York, 191–216, 1989.

[2] C. A. Felippa, "*A Survey of Parametrized Variational Principles and Applications to Computational Mechanics*," Comp. Meths. Appl. Mech. Engrg., **113**, 109–139, 1994.

[3] C. A. Felippa, "*Parametrized Unification of Matrix Structural Analysis: Classical Formulation and d-Connected Mixed Elements*," Fin. Elem. Anal. Des., **21**, 45–74, 1995.

[4] C. A. Felippa, "*Recent Developments in Parametrized Variational Principles for Mechanics*," Comput. Mech., **18**, 159–174, 1996.

[5] K. C. Park, G. W. Reich and K. F. Alvin, "*Damage Detection Using Localized Flexibilities*," in Structural Health Monitoring, Current Status and Perspectives, ed. by F.-K. Chang, Technomic Pub., 125–139, 1997.

[6] K. C. Park and G. W. Reich, "*A Theory for Strain-based Structural System Identification*, Proc. 9th International Conference on Adaptive Structures and Technologies, 14–16 October 1998, Cambridge, MA.

[7] P. G. Bergan and M. K. Nygård, "Finite Elements with Increased Freedom in Choosing Shape Functions," Int. J. Numer. Meth. Engrg., **20**, 643–664, 1984.

[8] C. A. Felippa, K. C. Park and M. R. Justino, "*The Construction of Free-Free Flexibility Matrices as Generalized Stiffness Inverses*," Computers & Structures, **68**, 411–418, 1998.

[9] C. A. Felippa and K. C. Park, "*The Construction of Free-Free Flexibility Matrices for Multilevel Structural Analysis*," Comp. Meths. Appl. Mech. Engrg., **191**, 2139–2168, 2002.

[10] B. M. Irons and S. Ahmad, "*Techniques of Finite Elements*," Ellis Horwood Ltd, 1980.

[11] P. G. Bergan and L. Hanssen, "*A New Approach for Deriving 'Good' Finite Elements*," in The Mathematics of Finite Elements and Applications – Volume II, ed. by J. R. Whiteman, Academic Press, London, 483–497, 1975.

[12] P. G. Bergan, "*Finite Elements Based on Energy Orthogonal Functions*," Int. J. Numer. Meth. Engrg., **15**, 1141–1555, 1980.

[13] C. Militello and C. A. Felippa, "*The First ANDES Elements: 9-DOF Plate Bending Triangles*," Comp. Meths. Appl. Mech. Engrg., **93**, 217–246, 1991.

[14] C. A. Felippa and C. Militello, "*Membrane Triangles with Corner Drilling Freedoms: II. The ANDES Element*," Fin. Elem. Anal. Des., **12**, 189–201, 1992.

[15] C. A. Felippa, "*Customizing the Mass and Geometric Stiffness of Plane Thin Beam Elements by Fourier Methods*," Engrg. Comput., **18**, 286–303, 2001.

[16] C. A. Felippa, "*Customizing High Performance Elements by Fourier Methods*," Trends in Computational Mechanics, ed. by W. A. Wall, K.-U. Bleitzinger and K. Schweizerhof, CIMNE, Barcelona, Spain, 283-296, 2001.